Ultrasound Transducer Models for Piezoelectric Polymer Films

LEWIS F. BROWN, MEMBER IEEE AND DAVID L. CARLSON, MEMBER IEEE

Abstract—**The frequency-dependent dielectric and mechanical losses of PVDF and P(VDF-TrFE) films demand special consideration for application of classical electromechanical circuit models. A method is presented for determining the piezoelectric constants and the frequency-dependent dielectric properties of the polymers from a five-step algorithm based on analysis of air-loaded broad-band impedance measurements. It is then shown how to account for the frequency-dependent lossy properties of these films in an equivalent impedance circuit model and a modified Mason's model. Comparisons between the models and actual film transducers show excellent broad-band simulation of both electrical input impedance and ultrasonic pulse-echo performance.**

I. Introduction

THE PURPOSE of this research was to develop an impedance-fit method for determining the piezoelectric and dielectric properties of piezoelectric polymer films, and to incorporate these properties into an electromechanical circuit model that accurately predicts the performance of ultrasound transducers. The authors were involved in analyzing unique samples of piezoelectric PVDF and P(VDF-TrFE), each manufactured under slightly different processing conditions. A simple method, preferably a computational procedure, was desired for determining the dielectric and piezoelectric properties of the polymer films with sufficient accuracy to make quantitative comparisons in ultrasound transducer performance.

The high dielectric and mechanical losses; and the frequency-dependent dielectric, elastic, and piezoelectric properties of these polymers demand special consideration in applying classical electromechanical circuit modeling techniques. The polymers have dielectric and elastic properties with large complex components that vary with both temperature and frequency [1]–[6].

A variety of methods has been previously reported for determining the acoustic and dielectric properties of the polymers based on fitting the theoretical and actual impedance/admittance measurements of free resonators [3], [7], [8]. However, insufficient details were reported in these works to formulate a step-by-step procedure for determining the material constants of interest. Other reported methods for determining the material properties of PVDF and lossy reasonators include iterative methods [1], [9] and impedance resonance methods [8], [10].

Various approaches have been reported for accounting for the dielectric and mechanical losses in transducer models for a lossy resonator. Ravinet *et al.* [11] included a dielectric loss resistance in their series equivalent resistance–inductance–capacitance (RLC) circuit for PVDF. Ohigashi *et al.* [12] and Kimura *et al.* [13] accounted for the dielectric and mechanical losses of piezoelectric polymers in Mason's model by including the imaginary components of dielectric permittivity and elastic stiffness. An intuitive approach taken by Rhyne [14] accounted for mechanical losses in Mason's model by adding a series resistance to the mechanical side of the circuit.

In this paper, we first describe a method for determining the frequency-dependent dielectric properties ϵ_{33} and $\tan \delta_e$ for the polymers. We then describe a method for determining the equivalent RLC circuit for PVDF and P(VDF-TrFE) thickness-mode vibrators operating near resonance. In the next section we describe our five-step procedure for determining f_s, f_p, Q_m, v_o, k_t, and our method of accounting for the polymers' lossy properties in a modified Mason's model. In the final section we include comparisons in actual pulse–echo transducer performance with that predicted with our modified Mason's model.

II. Modeling the Frequency-Dependent Dielectric Losses

The frequency-dependent dielectric losses of PVDF and P(VDF-TrFE) have been reported by many investigators [11], [15], [16]. These lossy properties play a key role in the low-Q broad-band acoustic performance of the polymers. The dielectric losses can be accounted for by making use of the complex dielectric constant $\epsilon_{33}^* = \epsilon_{33}(1 - j \tan \delta_e)$ [12], [13]. Since $\tan \delta_e$ represents the ratio of conduction current to displacement current in a dielectric, another classical approach that utilizes $\tan \delta_e$ to account for dielectric losses is to shunt the bulk capacitance of the film element, C_o, with a dielectric loss resistance, R_o, given by

$$C_o = \epsilon_{33} A/d \tag{1}$$

$$R_o = 1/\omega C_o \tan \delta_e \tag{2}$$

where A is the film area and d is the film thickness.

Both ϵ_{33} and $\tan \delta_e$ are frequency dependent for PVDF and P(VDF-TrFE) and are known to vary with the

Manuscript received March 15, 1988; revised and accepted November 28, 1988.

L. F. Brown and D. L. Carlson are with the Biomedical Engineering and Electrical Engineering Departments, Iowa State University, Ames, IA 50011.

IEEE Log Number 8926468.

0885-3010/89/0500-0313$01.00 © 1989 IEEE

stretching and poling conditions used [11]. It is possible to approximate ϵ_{33} and tan δ_e from simple electrical input impedance measurements by making use of the fact that at frequencies far from resonance, the input impedance is essentially due to that of C_o and R_o. This impedance can be written as

$$Z_{\text{in}} = R_o // C_o = R_o/(1 + j\omega C_o R_o). \quad (3)$$

By solving for the impedance magnitude, $|Z_{\text{in}}|$, and phase angle, θ_z, of (3) and substituting (1) and (2), expressions for ϵ_{33} and tan δ_e can be written as

$$\tan \delta_e = -1/(\tan(\theta_z)) \quad (4)$$

and

$$\epsilon_{33} = d/\{|Z_{\text{in}}|\, \omega A\, (\tan^2 \delta_e + 1)^{1/2}\}. \quad (5)$$

Thus, by knowing the physical dimensions of the film, one can approximate ϵ_{33} and tan δ_e from knowledge of the input impedance at frequencies far from resonance.

We fabricated a test fixture for air-backed film samples and, using an HP4815A RF impedance meter, acquired input impedance measurements over a broad frequency range that included the mechanical resonance frequency of the samples. The impedance measurements, corrected for stray capacitance and lead impedance, were used in a computer program that computed ϵ_{33} and tan δ_e from (4) and (5). Plots of these discrete measurements were made for each sample and showed the same behavior characteristic of the polymers [6], [11], [16], [17], except at frequencies near resonance. By making use of the fact that (4) and (5) are valid only at frequencies far from resonance, one can obtain close approximations for ϵ_{33} and tan δ_e near resonance by "smoothly" interpolating the program results through resonance as shown in Fig. 1. The solid lines in the plots represent the interpolated approximations for ϵ_{33} and tan δ_e for a 52-μ PVDF sample (Kynar Piezo Film, Pennwalt Corporation, Valley Forge, PA).

This procedure can be used to provide excellent first-order approximations for ϵ_{33} and tan δ_e for PVDF. We later show how to further tune these approximations for increased accuracy.

III. Simplified Impedance Model

Fig. 2 shows the classical electrical circuit used to model the input impedance of a lossy piezoelectric resonator operating near resonance. The series resonant branch of R_s, L_s, and C_s represents the effects of series resonance on the input impedance.

To model the electrical input impedance of air-backed PVDF, we began by using our previously derived approximations for ϵ_{33} and tan δ_e to compute R_o and C_o. Thus, completion of the model required derivation of the series resonance branch. These component values may be easily derived if the impedance of the branch, Z_s, is available at several frequencies near resonance. Since the piezoelectric polymers have high dielectric losses and low k_{eff} values (i.e., $k_{\text{eff}}^2 Q < 1$) caution must be used in modeling Z_s, as clearly noted in the IEEE standards [18]. The frequency dependence of their dielectric, elastic, and piezoelectric properties compounds the need to exercise care. Their low figure of merit ($M < 1$) is evident in their highly damped air-loaded impedance/admittance near resonance, where the series and parallel resonance frequencies are obscured.

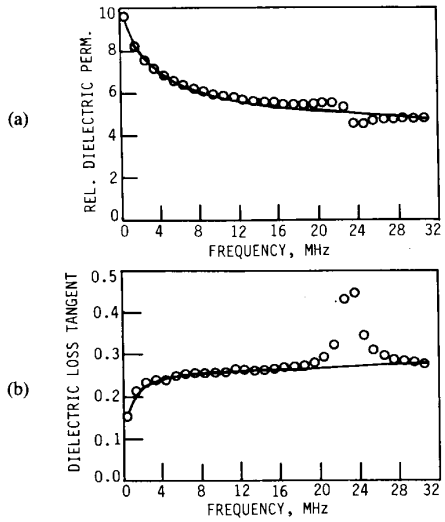

Fig. 1. Discrete points represent program results for 52-μ PVDF using (1) and (2). Continuous lines represent results after "smoothly" interpolating through resonance (23 MHz). (a) Interpolated plots of relative dielectric permittivity, ϵ_{33}. (b) Interpolated plots of dielectric loss tangent, tan δ_e.

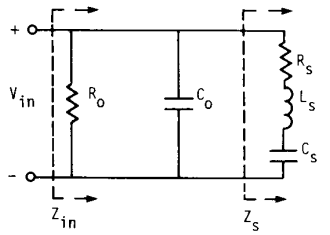

Fig. 2. Equivalent circuit for lossy piezoelectric resonator near resonance.

To derive the series resonance components, a computer program was used to compute Z_s by removing the shunt impedance of R_o and C_o from actual input impedance measurements. The Fortran program used complex algebra to: 1) convert the measured input impedance, Z_{in}, to an admittance, Y_{in}, 2) subtract the admittance of R_o in shunt with C_o, and 3) convert the remaining admittance to the desired impedance, Z_s. By analyzing Z_s near resonance the components R_s, L_s, and C_s were computed.

Series resonance, ω_s, can be approximated by noting where the imaginary part of Z_s, jX_s, crosses 0Ω. One can thus compute L_s and C_s by equating the imaginary part of Z_s to the series reactance, $\omega L_s - 1/\omega C_s$, at two frequencies near series resonance. This approach forces the input impedance of the model to fit the actual measurements at these two frequencies. To better fit the model and actual measured impedances over a wider frequency range, L_s

and C_s were instead chosen to match the slope of X_s over a frequency range symmetric about resonance. This can be done by noting

$$\omega_s = 1/(L_s C_s)^{1/2} \tag{6}$$

and

$$X_s(\omega) = \omega L_s - 1/\omega C_s \tag{7}$$

thus

$$\Delta X_s = X_s(\omega + \Delta\omega) - X_s(\omega) \tag{8}$$

$$\Delta X_s = [(\omega + \Delta\omega) L_s - 1/(\omega + \Delta\omega) C_s] - [\omega L_s - 1/\omega C_s]. \tag{9}$$

By substituting (6) into (9) for L_s, the value of C_s that matches the slope of X_s, $\Delta X_s(\omega)/\Delta\omega$, to the actual measurements is

$$C_s = \frac{\Delta\omega}{\Delta X_s(\omega)} \left[\frac{1}{\omega_s^2} + \frac{1}{\omega(\omega + \Delta\omega)} \right]. \tag{10}$$

The slope of X_s can be computed from a linear regression of the program results for X_s, determined from discrete measurements of Z_s in the neighborhood of series resonance, and C_s then computed from (10). (6) is then used to compute L_s and the mechanical resistance, R_s, is taken from a linear interpolation of the real part of Z_s at resonance (i.e., $Re(Z_{in})$ where $X_s = 0$).

This approach was used to derive the simplified impedance model for our 52-μ PVDF sample. The series resonance components L_s (30.38 μH) and C_s (1.59 pF) were chosen to match the slope of X_s to that of the actual measurements over the 1-MHz frequency range symmetric about resonance (22.9 MHz). The mechanical Q of the Z_s branch (11.3) was computed from

$$Q_s = 1/\omega_s R_s C_s$$

where

$$R_s = 388.0\ \Omega.$$

The input impedance of the completed model was computed and compared with the actual impedance measurements over a broad frequency range. Fig. 3 shows the results near resonance. The simplified impedance model results deviated less than 2 percent from the actual impedance magnitude and phase measurements over a frequency range of 0.5–32 MHz.

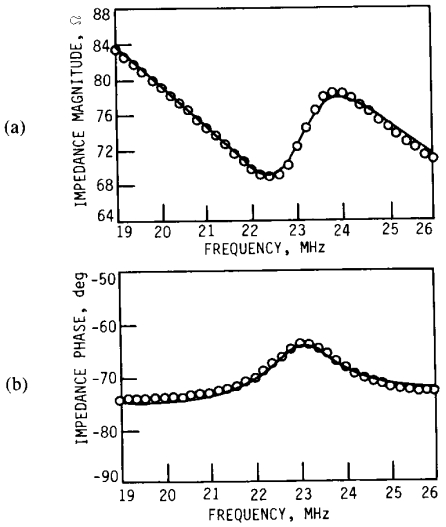

Fig. 3. Comparison of actual input impedance measurements and simplified model results near resonance. (a) Impedance magnitude. (b) Impedance phase.

IV. Complete Electromechanical Model

Many investigators have used Mason's classical circuit model [19] to analyze the electromechanical behavior of acoustic resonators [20]–[22], [25]. Persson and Hertz [24] have shown the value in using an inverse fast Fourier transform (FFT) on the Mason's model transfer function to compute pulse shapes for thickness-mode ceramic transducers.

Mason's model derivation was based on negligible dielectric and mechanical losses—suitable assumptions for dealing with most known piezoelectric materials at the time of his now classical work. Materials with high dielectric and mechanical losses such as PVDF cannot be accurately analyzed with Mason's model without modifying the circuit to account for these losses. To account for the frequency-dependent dielectric losses of PVDF, the dielectric portion of Mason's model can be replaced by our previously derived shunt combination of R_o and C_o. The complex elastic and piezoelectric properties of the polymers, known to vary with both frequency and temperature, must be taken into account for exact modeling of electromechanical behavior. In our attempt to approximate their electromechanical behavior we used a frequency-independent value for Q_m (i.e., $1/\tan\delta_m$) and a real valued electromechanical transformer coefficient, ϕ. Using our methods, these values are easily determined at resonance. To account for the high mechanical losses we chose an approach similar to Rhyne [14]. A mechanical-loss resistance, R_m, was added to the Mason's model as shown in Fig. 4.

To compute the remaining components of the circuit requires knowledge of R_m, C_m, Q_m, v_0, and k_t. By using our algorithm, all of these parameters may be derived from air-loaded input impedance measurements and knowledge of the physical quantities A, d, and ρ.

R_o	$1/(\omega C_o \tan\delta_e)$, dielectric loss resistance.
C_o	$\epsilon_{33} A/d$, bulk capacitance.
ρ	density.
v_o	sound velocity.
R_m	mechanical loss resistance.
C_M	mechanical capacitance.
Q_M	$1/\omega R_M C_M$, air-loaded mechanical Q.
Z_o	ρv_o, acoustic impedance of piezoelectric material.
Z_E	ρv_E, acoustic impedance of electrodes.
Z_F, Z_B	acoustic impedance of front, rear load.

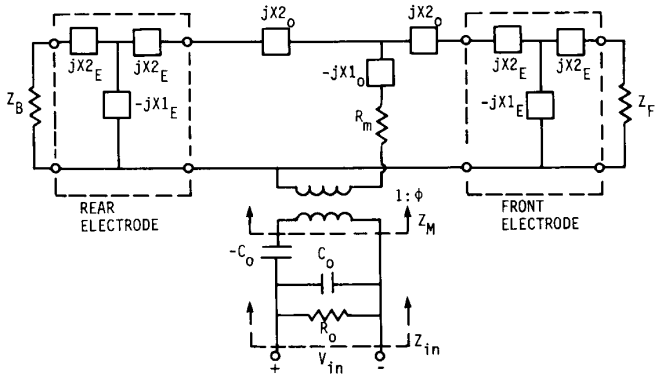

Fig. 4. Modified Mason's model for PVDF, P(VDF-TrFE).

$X1_n$ $Z_n/\sin(\theta_n)$.
$X2_n$ $Z_n \tan(\theta_n/2)$.
θ $2\pi fd/v$.
f frequency (Hz).
ϕ $k_t[v_o C_o Z_o/d]^{1/2}$.
k_t electromechanical coupling coefficient.

Before beginning the algorithm, we use an approach similar to that in deriving the components of the simplified impedance model. The impedance $\bar{Z}_M$, $(\bar{R}_M + j\bar{X}_M)$, is computed by removing the shunt impedance of R_o and C_o, and the impedance of the negative capacitance, $-C_o$, from the actual input impedance measurements near resonance. This remaining impedance is compared to the theoretical model's value Z_M, $(R_M + jX_M)$, where

$$R_M = (R_m + Z/2)/\phi^2 \qquad (11)$$

and Z is the acoustic impedance of air at the front/rear loads (neglecting the electrode layers). The remaining model parameters are determined from the forthcoming algorithm.

1) The parallel resonant frequency f_p, is determined from a linear interpolation of the discrete frequency values for $j\bar{X}_M = 0$. The acoustic velocity of the film, v_0, can then be determined from $v_0 = 2df_p$.
2) The slope, $\Delta\bar{X}_M(\omega)/\Delta\omega$, is computed in the 1-MHz frequency range symmetric about f_p, and C_M is computed from (10).
3) $\bar{R}_M$ is then determined from a linear interpolation of Real $\{\bar{Z}_M\}$ at f_p.
4) The computer-generated theoretical impedance, Z_M, is then compared with $\bar{Z}_M$, and Q_M is set to match $\bar{R}_M$ with R_M at resonance. R_m is then determined from (11).
5) Finally, k_t is set to match the theoretical model's slope, $\Delta X_M(\omega)/\Delta\omega$, with the measured value of step (2) in the 1-MHz frequency range symmetric about f_p.

The algorithm can be easily implemented in a computer program, making the component computations relatively easy. We used this modeling approach to analyze numerous PVDF and P(VDF-TrFE) film samples. For the 52 micron PVDF sample our analysis gave $Q_M = 11.6$ and $k_t = 14.6$ percent at parallel resonance. In all cases our computed values for Q_M and k_t were in excellent agreement with the manufacturer's specifications. Fig. 5 shows the comparison between the input impedances of our modified Mason's model and the actual measurements in the neighborhood of resonance. The model deviated less than 1 percent from the actual impedance measurements over a frequency range of 0.5–32 MHz.

The values for ϵ_{33} and tan δ_e were derived by assuming that at frequencies far from resonance, the input impedance is essentially due to C_o shunted by R_o. The model results show that this is indeed the case, however, the mechanical portion of the model always exhibits some, even if negligible, effect on the input impedance. Thus, after computing the wide-band deviation of the input impedance of the model and actual measurements, one can "tune" the ϵ_{33} and tan δ_e values to shift the deviation to zero, and recompute the circuit components using our algorithm. A computer program can be used to perform such iterations until the magnitude of the impedance deviations lies within the uncertainty of the actual impedance measurements. The result is a model that best fits the measured impedance values.

V. Electromechanical Model Simulations

The real value of an accurate electromechanical transducer model is not in predicting input impedance, but rather in predicting the ultrasonic performance of a particular transducer design. We have incorporated our modified Mason's model into a menu-driven interactive transducer design/simulation program. Under careful experimental conditions the program provides excellent prediction of transducer performance.

We used our modeling algorithm to analyze P(VDF-TrFE) film (110 micron thickness, 300-Å gold metallized electrodes) and then carefully constructed broad-band test probes with acoustically matched backings. The probes were submersed in a scanning tank and excited by a commercial pulser (Panametrics 5052PR). Pulse-echo reflections from a fused silica target in the near field (normal

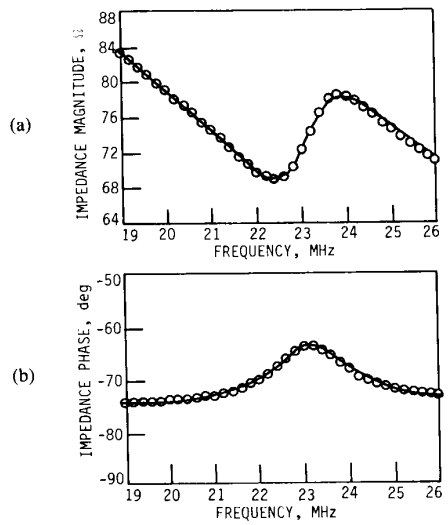

Fig. 5. Comparison of actual impedance measurements and modified Mason's model results near resonance. (a) Impedance magnitude. (b) Impedance phase.

incidence) were digitized on a high-speed sampling system (Le Croy 9400). The transducer-loaded input pulse waveforms were also sampled and stored for convolution with our model in the simulation program.

The program computes the 512-point FFT of the actual input pulse waveform, evaluates the pulse-echo performance of the model in the frequency domain, and finally computes the time domain response with an inverse FFT. The precise target distance is used to correct the results for diffraction and reflection. Fig. 6 shows a comparison between the actual sampled pulse-echo waveform and the pulse waveshape predicted with the model.

It should be noted here that such good correlation in the actual and predicted results is likely to occur only if careful attention is given to accurately accounting for all impedances of the measurement system. Since the piezoelectric polymer films have inherently low capacitance, the capacitance of the connecting cables and receiver must be considered for any meaningful prediction of actual performance. Equally important are accounting for the gain and damping of the receiver, and precise normal incidence focussing on the target. By measuring and accounting for all of these experimental considerations, our modified Mason's model has provided excellent predictions of PVDF and P(VDF-TrFE) probes with both voltage impulse and voltage step function inputs.

VI. Conclusion

A method has been presented for modeling the electromechanical performance of PVDF and P(VDF-TrFE) ultrasound transducers. By properly accounting for the frequency-dependent dielectric properties and mechanical losses of the polymers, a modified Mason's model can be used to accurately predict input impedance and ultrasonic performance. The piezoelectric constants needed for the modeling are found by following a five-step algorithm based on evaluating air-loaded electrical input impedance measurements. Our modeling technique has proven to be especially useful in using computer simulations to assess prototype designs for broad-band PVDF and P(VDF-TrFE) probes.

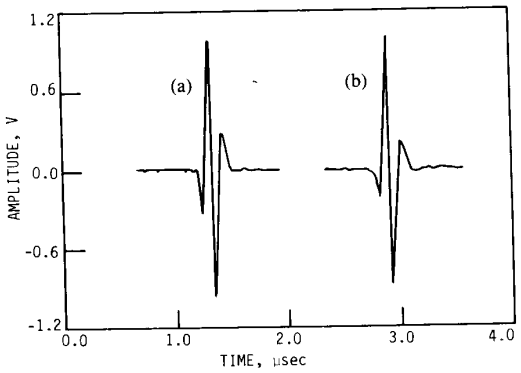

Fig. 6. P(VDF-TrFE) pulse-echo waveforms from a fused silica target. (a) Actual waveform. (b) Waveform predicted with author's modified Mason's model.

Acknowledgment

The authors would like to thank Pennwalt Corporation Piezo Film Department, especially Kumar Ogale, for providing the high-quality films used in this research. We would also like to express our gratitude to the Ames Laboratory and Center for NDE, Iowa State University; particularly D. K. Hsu, D. O. Thompson, and S. J. Wormley for the use of their testing facilities and valued interest and support.

References

[1] Q. C. Xu, A. R. Ramachandran, R. E. Newnham, and R. H. Tancrell, "Measurement of complex coefficients for thick PVDF polymer," in *Proc. 1987 IEEE Ultrason. Symp.*, 1987, pp. 663-666.

[2] H. Ohigashi and K. Koga, "Ferroelectric copolymers of vinylidene-fluoride and trifluoethylene with a large electromechanical coupling factor," *Jap. J. Appl. Phys.*, vol. 21, no. 8, pp. L455-L457, Aug. 1982.

[3] K. Koga and H. Ohigashi, "Piezoelectricity and related properties of vinylidene fluoride and trifluoroethylene copolymers," *J. Appl. Phys.*, vol. 59, no. 6, pp. 2142-2150, Mar. 1986.

[4] H. Yamazaki, J. Ohwaki, T. Yamada, and T. Kitayama, "Temperature dependence of the pyroelectric response of vinylidene fluoride trifluorethylene copolymer and the effect of its poling conditions," *Appl. Phys. Letters*, vol. 39, no. 9, pp. 772-773, Nov. 1, 1981.

[5] E. Fukada and T. Furakawa, "Piezoelectricity and ferroelectricity in polyvinylidene fluoride," *Ultrason.*, vol. 19, no. 1, pp. 31-39, Jan. 1981.

[6] G. M. Sessler, "Piezoelectricity in polyvinylidene fluoride," *J. Acoust. Soc. Am.*, vol. 70, no. 6, pp. 1596-1608, Dec. 1981.

[7] H. Ohigashi, "Electromechanical properties of polarized polyvinylidene fluoride films as studied by the piezoelectric resonance method," *J. Appl. Phys.*, vol. 47, no. 3, pp. 949-955, Mar. 1976.

[8] S. Saitoh *et al.*, "The method of determining K_t and Q_m for low Q piezoelectric materials," in *Proc. 1985 Ultrason. Symp.*, 1985, pp. 620-623.

[9] J. G. Smits, "Iterative method for accurate determination of the real and imaginary parts of the materials coefficients of piezoelectric ceramics," *IEEE Trans. Son. Ultrason.*, vol. SU-23, no. 6, pp. 393-402, Nov. 1976.

[10] L. N. Bui, H. J. Shaw, and L. T. Zitelli, "Study of acoustic wave

resonance in piezoelectric PVF_2 film," *IEEE Trans. Son. Ultrason.*, vol. SU-24, no. 5, pp. 331-336, 1977.
[11] P. Ravinet *et al.*, "Acoustic and dielectric loss processes in PVF2," *Proc. 1980 IEEE Ultrason. Symp.* 1980, pp. 1017-1022.
[12] H. Ohigashi *et al.*, "Piezoelectric and ferroelectric properties of P(VDF-TrFE) copolymers and their application to ultrasonic transducers," *Ferroelec.*, vol. 60, pp. 263-276, 1984.
[13] K. Kimura, N. Hashimoto, and H. Ohigashi, "Performance of a linear array transducer of vinylidene fluoride trifluoroethylene copolymer," *IEEE Trans. Son. Ultrason.*, vol. SU-32, no. 4, pp. 566-572, July 1985.
[14] T. L. Rhyne, "An improved interpretation of Mason's model for piezoelectric plate transducers," *IEEE Trans. Son Ultrason.*, vol. SU-25, no. 2, pp. 98-103, March 1978.
[15] R. G. Swartz and J. D. Plummer, "Monolithic silicon-PVDF piezoelectric arrays for ultrasonic imaging," *Acoust. Imaging*, vol. 8, A. F. Metherall, Ed. New York: Plenum, 1980, pp. 69-95.
[16] J. W. Hunt, M. Arditi, and F. S. Foster, "Ultrasound transducers for pulse-echo medical imaging," *IEEE Trans. Biomed. Eng*, vol. BME-300, no. 8, pp. 453-481, 1983.
[17] R. G. Swartz and J. D. Plummer "On the generation of high-frequency acoustic energy with polyvinylidene fluoride," *IEEE Trans. Son. Ultrason.*, vol. SU-27, no. 6, pp. 295-302, Nov. 1980.
[18] "IEEE Standard on Piezoelectricity," *IEEE Trans. Son. Ultrason.*, vol. SU-31, no. 2, Mar. 1984.
[19] W. P. Mason, *Electromechanical Transducers and Wave Filters*, 2nd ed. New York: Van Nostrand, 1948, pp. 185-224.
[20] G. Kossoff, "The effects of backing and matching on the performance of piezoelectric ceramic transducers," *IEEE Trans. Son. Ultrason.*, vol. SU-13, no. 1, pp. 20-31, 1966.
[21] C. T. Lancee, J. Souquet, H. Ohigashi, and N. Bom, "Ferroelectric ceramics versus polymer piezoelectric materials," *Ultrason.*, vol. 23, no. 3, pp. 138-142, 1985.
[22] S. A. Morris and C. G. Hutchens, "Implementation of Mason's model on circuit analysis programs," *IEEE Trans. Ultrason. Ferroelec. Freq. Contr.*, vol. UFFC-33, pp. 295-298, 1986.
[23] T. Sato, K. Loyama, S. Ikeda, and T. Wada, "Short pulse response of ultrasonic transducer made of piezoelectric copolymer films of vinylidene fluoride-trifluoroethylene," *Jap. J. Appl. Phys.*, vol. 26, Supplement 26-1, pp. 100-102, 1986.
[24] H. W. Persson and C. H. Hertz, "Acoustic impedance matching of medical ultrasound transducers," *Ultrason.*, vol. 23, no. 2, pp. 83-89, 1985.
[25] M. G. Silk, *Ultrasonic Transducers for Nondestructive Testing*, Bristol: Adam Hilger Ltd., 1984, pp. 25-109.

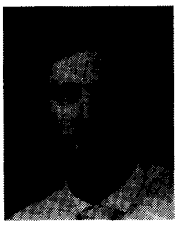

Lewis F. Brown (S'81-M'88) was born in Arlington, VA on June 8, 1953. He received the B.S.E.E. from South Dakota State University, Brookings, in 1984, the M.S.E.E. and the Ph.D. degrees in biomedical engineering and electrical engineering from Iowa State University, Ames, in 1986 and 1988, respectively.

Following four years of experience as a laboratory technician in the U.S. Air Force, he was employed as biomedical engineering technician for four years, and a clinical engineer for four years. While pursuing his graduate degrees at Iowa State University, he taught courses in electrical engineering and lectured in signal processing techniques for biomedical engineering. He is currently Senior Research Scientist and head of ultrasound research and development for Pennwalt Corporation Piezo Film Department in Valley Forge, PA. His current interests are in ultrasound transducer design, modeling, fabrication, and testing.

Dr. Brown is a member of the IEEE Societies of Engineering in Medicine and Biology; Ultrasonics, Ferroelectrics, and Frequency Control; and Education. He is also a member of Eta Kappa Nu, Tau Beta Pi, Phi Kappa Phi, and the American Society for Engineering Education.

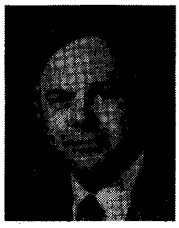

David L. Carlson (S'60-M'65) was born in Minneapolis, MN. He received the B.S.E.E. degree from the University of Minnesota, Minneapolis, in 1959, and the Ph.D. degree in electrical engineering from Iowa State University, Ames, in 1964.

He is an Associate Professor of electrical engineering at Iowa State University and a faculty member at the Biomedical Engineering Program. His current research activity is in ultrasonics.